

PAPER

Five momenta

To cite this article: M V Berry 2013 *Eur. J. Phys.* **34** 1337

View the [article online](#) for updates and enhancements.

Related content

- [Photon trajectories, anomalous velocities and weak measurements: a classical interpretation](#)
Konstantin Y Bliokh, Aleksandr Y Bekshaev, Abraham G Kofman et al.
- [Optical currents](#)
M V Berry
- [Fast Track Communication](#)
M V Berry and M R Dennis

Recent citations

- [Quantum mechanics and classical light](#)
Thomas Konrad and Andrew Forbes
- ["Plasmonics" in free space: observation of giant wavevectors, vortices, and energy backflow in superoscillatory optical fields](#)
Guanghui Yuan *et al*
- [Geometry of 3D monochromatic light: local wavevectors, phases, curl forces, and superoscillations](#)
M V Berry and Pragya Shukla



IOP | ebooks™

Bringing you innovative digital publishing with leading voices to create your essential collection of books in STEM research.

Start exploring the collection - download the first chapter of every title for free.

Five momenta

M V Berry

H H Wills Physics Laboratory, Tyndall Avenue, Bristol BS8 1TL, UK

E-mail: asymptotico@bristol.ac.uk

Received 3 June 2013, in final form 10 July 2013

Published 23 August 2013

Online at stacks.iop.org/EJP/34/1337

Abstract

A quantum or classical wavefunction depending on position can be associated with a local momentum in at least five apparently different ways: first, as the phase gradient of the wavefunction; second, as the local expectation value of the momentum operator; third, via the local current; fourth, via the Wigner phase-space distribution function; and fifth, as the weak value of momentum with position postselected. The different formulas are all equivalent, but give different insights into the underlying physics. Momenta one through three are largely familiar, but the fourth and fifth are less so.

(Some figures may appear in colour only in the online journal)

1. Introduction

The theories of physics are multiply connected, in the sense that a given concept associated with them can often appear to originate in very different yet ultimately equivalent ways. Understanding this gives flexibility in applying the theories, so it would seem useful to include examples when teaching physics. The example I explore in this paper is the concept of local momentum.

Consider a quantum particle moving in D dimensions, described by its wavefunction in position representation, or a classical wave, namely

$$\langle \mathbf{r} | \psi \rangle = \psi(\mathbf{r}), \quad \mathbf{r} = \{x_1, x_2, \dots, x_D\}. \quad (1.1)$$

The emphasis in this paper will be on the momenta associated with the state $|\psi\rangle$. It will be convenient to use units in which Planck's constant $\hbar = 1$; this is equivalent to working with the wavenumber \mathbf{k} , which is also more natural for classical waves, e.g. in optics. Only for the case of a single plane wave does $|\psi\rangle$ correspond to a unique value of \mathbf{k} . For any other wavefunction, there is a distribution of momenta, described by the momentum representation

$$\langle \mathbf{k} | \psi \rangle = \bar{\psi}(\mathbf{k}) = \frac{1}{(2\pi)^{D/2}} \int_{\text{space}} d\mathbf{r} \exp(-i\mathbf{k} \cdot \mathbf{r}) \psi(\mathbf{r}). \quad (1.2)$$

However, with $\bar{\psi}(\mathbf{k})$ the immediate accessibility of the position information is lost, and this is reinforced by the uncertainty relation: it is impossible to specify uniquely the momentum at

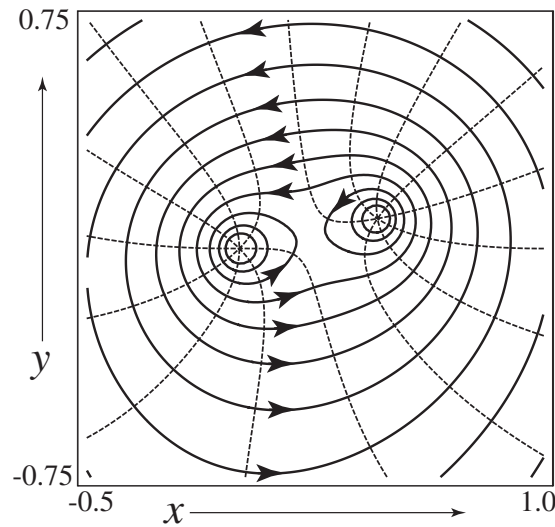


Figure 1. Momentum vectors $\mathbf{k}_{\text{phase}}(x,y)$ (curves with arrows), orthogonal to the wavefronts $\arg \psi$ (dashed curves at phase intervals of $\pi/4$), for $\psi(\mathbf{r}) = z - 2z^2 + iz^3$, ($z = x + iy$). (Since this special case is an analytic function of x and y , the momentum lines are easily computed as contours of $|\psi|$.)

any given position. Nevertheless, it is natural to ask: is there a way to define a *local momentum* $\mathbf{k}(\mathbf{r})$, that would encapsulate in a useful way at least part of the momentum information contained in $\psi(\mathbf{r})$? The answer is yes—and there are at least five such ways. Moreover, they are all equivalent. The equivalences are sometimes almost trivial, sometimes less so. But each of the formulations gives a different insight into the state $|\psi\rangle$, so it seems worthwhile to present and compare them. That is my purpose here.

The first three of the five ways of representing local momentum are mostly standard material. The fourth and fifth, making connections with Wigner functions (section 5) and weak measurement theory and superoscillations (section 6) are less familiar.

2. Momentum 1: local phase gradient

Implicit in our replacement of momentum by the wavevector \mathbf{k} is the de Broglie association between wave physics and particle mechanics. This suggests defining the first and perhaps simplest of our local momenta as the gradient of the phase of $\psi(\mathbf{r})$, giving:

$$\mathbf{k}_{\text{phase}}(\mathbf{r}) = \nabla \arg[\psi(\mathbf{r})] = \nabla \text{Im}[\log \psi(\mathbf{r})] = \text{Im} \frac{\nabla \psi(\mathbf{r})}{\psi(\mathbf{r})}. \quad (2.1)$$

Thus, as illustrated in figure 1, the vector $\mathbf{k}_{\text{phase}}(\mathbf{r})$ is perpendicular to the wavefronts, which are the constant-phase manifolds of $\psi(\mathbf{r})$ (lines for $D = 2$, surfaces for $D = 3$).

When divided by the mass of the quantum particle, the phase gradient plays a central role in Madelung's hydrodynamic interpretation [1], as the velocity of a fluid envisaged to be driven by the wavefunction. Reinterpreted as the velocity of individual particles, the same quantity lies at the basis of the de Broglie–Bohm interpretation [2] of quantum mechanics. In optical diffraction, described in terms of a scalar wave (see section 7 for more discussion of this), $\mathbf{k}_{\text{phase}}$ can be regarded as defining the direction of ‘rays’—paths of particles of light as envisaged by Newton—and (as I have discussed in more detail elsewhere [3]) makes

retrospective sense of his enigmatic speculation [4] about diffraction fringes associated with edge diffraction: ‘Are not the rays of Light, in passing by the edges and sides of Bodies, bent several times backwards and forwards, with a motion like that of an Eel? And do not the three Fringes of Colour’d Light above-mentioned arise from three such bendings?’

3. Momentum 2: local operator

The usual expectation value of an operator \hat{A} in the state $|\psi\rangle$ is

$$A_{\text{expectation}} = \langle \psi | \hat{A} | \psi \rangle = \int d^D \mathbf{r} \int d^D \mathbf{r}' \psi^*(\mathbf{r}) \langle \mathbf{r} | \hat{A} | \mathbf{r}' \rangle \psi(\mathbf{r}'), \quad (3.1)$$

involving $\psi(\mathbf{r})$ over the whole space \mathbf{r} . A natural way to define a corresponding quantity that is localized at a specified position \mathbf{r} and normalized is

$$A_{\text{local operator}}(\mathbf{r}) = \frac{\langle \psi | \frac{1}{2} (\delta(\mathbf{r} - \hat{\mathbf{r}}) \hat{A} + \hat{A} \delta(\mathbf{r} - \hat{\mathbf{r}})) | \psi \rangle}{\langle \psi | \delta(\mathbf{r} - \hat{\mathbf{r}}) | \psi \rangle}, \quad (3.2)$$

in which the symmetrization is necessary because the operators \hat{A} and $\hat{\mathbf{r}}$ generally do not commute.

When applied to momentum, this gives the second of our formulas:

$$\mathbf{k}_{\text{local operator}}(\mathbf{r}) = \frac{\langle \psi | \frac{1}{2} (\delta(\mathbf{r} - \hat{\mathbf{r}}) \hat{\mathbf{k}} + \hat{\mathbf{k}} \delta(\mathbf{r} - \hat{\mathbf{r}})) | \psi \rangle}{\langle \psi | \delta(\mathbf{r} - \hat{\mathbf{r}}) | \psi \rangle}. \quad (3.3)$$

It seems likely that this localized version of an operator (or at least the numerator) has been discovered independently several times. The earliest reference I can find is by Landau [5], who used it in his classic study of superfluid helium II. I made use of it in 1980 in connection with the Aharonov–Bohm effect [6].

The first of our equivalences is

$$\mathbf{k}_{\text{local operator}}(\mathbf{r}) = \mathbf{k}_{\text{phase}}(\mathbf{r}). \quad (3.4)$$

One way to show this is to use the position representation in (3.3), in which the momentum operator has the form

$$\hat{\mathbf{k}} = -i\nabla, \quad (3.5)$$

leading to the last of the equalities in (2.1).

4. Momentum 3: local current

Using the position representation (3.5) for the momentum operator, it follows [7] that the momentum current flowing out of a region bounded by a surface S is

$$\mathbf{J} = \int \int_S d\mathbf{S} \cdot \text{Im}[\psi^*(\mathbf{r}) \nabla \psi(\mathbf{r})]. \quad (4.1)$$

The integral can be represented in terms of the local momentum (current) density

$$\mathbf{j}(\mathbf{r}) = \text{Im}[\psi^*(\mathbf{r}) \nabla \psi(\mathbf{r})], \quad (4.2)$$

which suggests defining a local momentum by dividing by the density. Thus we have the third formula:

$$\mathbf{k}_{\text{current}}(\mathbf{r}) = \frac{\mathbf{j}(\mathbf{r})}{|\psi(\mathbf{r})|^2} = \frac{\text{Im}[\psi^*(\mathbf{r}) \nabla \psi(\mathbf{r})]}{|\psi(\mathbf{r})|^2}. \quad (4.3)$$

The next equivalence in our sequence is

$$\mathbf{k}_{\text{current}}(\mathbf{r}) = \mathbf{k}_{\text{local operator}}(\mathbf{r}) = \mathbf{k}_{\text{phase}}(\mathbf{r}). \quad (4.4)$$

This follows from including the denominator $|\psi(\mathbf{r})|^2$ inside the $\text{Im}[\dots]$ and then cancelling the functions $\psi^*(\mathbf{r})$.

5. Momentum 4: local Wigner average

One way to represent $|\psi\rangle$ directly in terms of \mathbf{r} and \mathbf{k} is through Wigner's phase-space distribution function. This is most simply written as the expectation value

$$W(\mathbf{r}, \mathbf{k}) = \langle \psi | \delta(\hat{X} - X) | \psi \rangle \quad (X \equiv \{\mathbf{r}, \mathbf{k}\}), \quad (5.1)$$

in which the D -dimensional operator δ function is defined by

$$\delta(\hat{X} - X) = \frac{1}{(2\pi)^D} \int d^D \mathbf{R} \int d^D \mathbf{K} \exp\{i((\hat{\mathbf{r}} - \mathbf{r}) \cdot \mathbf{K} + (\hat{\mathbf{k}} - \mathbf{k}) \cdot \mathbf{R})\}. \quad (5.2)$$

Easy manipulations give the more familiar form [8–10]

$$W(\mathbf{r}, \mathbf{k}) = \frac{1}{\pi^D} \int d^D \mathbf{R} \psi^*(\mathbf{r} + \mathbf{R}) \psi(\mathbf{r} - \mathbf{R}) \exp(2i\mathbf{k} \cdot \mathbf{R}). \quad (5.3)$$

This seems to privilege position over momentum, but since (5.1) is manifestly democratic in \mathbf{r} and \mathbf{k} there is an equivalent representation in terms of $\bar{\psi}(\mathbf{k})$. The Wigner function has the well-known properties that its projection along \mathbf{k} gives the intensity of the wave at \mathbf{r} , and vice versa:

$$\int d^D \mathbf{k} W(\mathbf{r}, \mathbf{k}) = |\psi(\mathbf{r})|^2, \quad \int d^D \mathbf{r} W(\mathbf{r}, \mathbf{k}) = |\bar{\psi}(\mathbf{k})|^2. \quad (5.4)$$

In terms of W , it is natural to define a local momentum—the fourth of our five—by

$$\mathbf{k}_{\text{Wigner}}(\mathbf{r}) = \frac{\int d^D \mathbf{k} \mathbf{k} W(\mathbf{r}, \mathbf{k})}{\int d^D \mathbf{k} W(\mathbf{r}, \mathbf{k})}. \quad (5.5)$$

The next in our sequence of equivalences is:

$$\mathbf{k}_{\text{Wigner}}(\mathbf{r}) = \mathbf{k}_{\text{current}}(\mathbf{r}) = \mathbf{k}_{\text{local operator}}(\mathbf{r}) = \mathbf{k}_{\text{phase}}(\mathbf{r}). \quad (5.6)$$

The simplest derivation is to use the representation (5.3) and show the equality with (4.3). For the denominator in (5.5), we use the first equality in (5.4). For the numerator, the derivation proceeds as follows:

$$\begin{aligned} \int d^D \mathbf{k} \mathbf{k} W(\mathbf{r}, \mathbf{k}) &= \frac{1}{\pi^D} \int d^D \mathbf{R} \psi^*(\mathbf{r} + \mathbf{R}) \psi(\mathbf{r} - \mathbf{R}) \int d^D \mathbf{k} \mathbf{k} \exp(2i\mathbf{k} \cdot \mathbf{R}) \\ &= \frac{1}{\pi^D} \int d^D \mathbf{R} \psi^*(\mathbf{r} + \mathbf{R}) \psi(\mathbf{r} - \mathbf{R}) \left(-\frac{\pi^D}{2} \right) i \nabla_{\mathbf{R}} \delta(\mathbf{R}) \\ &= \frac{i}{2} \int d^D \mathbf{R} \delta(\mathbf{R}) \nabla_{\mathbf{R}} [\psi^*(\mathbf{r} + \mathbf{R}) \psi(\mathbf{r} - \mathbf{R})] \\ &= \frac{i}{2} [(\nabla \psi^*(\mathbf{r})) \psi(\mathbf{r}) - \psi^*(\mathbf{r}) \nabla \psi(\mathbf{r})] = \text{Im} \psi^*(\mathbf{r}) \nabla \psi(\mathbf{r}). \end{aligned} \quad (5.7)$$

Two slightly unfamiliar Wigner functions, relevant to wave physics, will now be described. The first is a superposition of plane waves with different momenta \mathbf{k} , that is

$$\psi(\mathbf{r}) = \sum_{n=1}^N c_n \exp(i\mathbf{k}_n \cdot \mathbf{r}), \quad (5.8)$$

in which c_k are arbitrary complex coefficients. (For monochromatic fields, all the wavevector lengths $|\mathbf{k}|$ are the same, but the results to follow are more general.) From (5.3), the corresponding Wigner function is

$$\begin{aligned} W(\mathbf{r}, \mathbf{k}) &= \sum_{n=1}^N |c_n|^2 \delta(\mathbf{k} - \mathbf{k}_n) + \\ &2 \sum_{1 \leq m < n < N} \sum \delta\left(\mathbf{k} - \frac{1}{2}(\mathbf{k}_m + \mathbf{k}_n)\right) \text{Re}[c_m^* c_n \exp(i(\mathbf{k}_n - \mathbf{k}_m) \cdot \mathbf{r})]. \end{aligned} \quad (5.9)$$

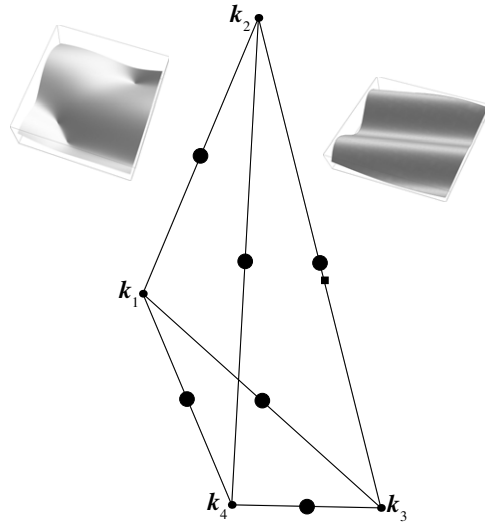


Figure 2. A four-wave superposition of the form (5.8) with random wavevectors k_n (small filled circles in the central panel, with the small square indicating $k = 0$), and random coefficients. The wave intensity $|\psi(\mathbf{r})|^2$ is shown as a surface in the left panel, over a range of x of y in which there are two nodal points (= phase singularities = wave vortices). Large filled circles in the central panel denote the midpoints between pairs of the contributing k_n , which are the momenta \mathbf{k} on which the Wigner function (5.9) is concentrated. Lines joining pairs of k_n represent the wavevectors in the corresponding trigonometric contributions to $W(\mathbf{r}, \mathbf{k})$ from each pair, one of which (corresponding to the pair k_2, k_3) is illustrated as a surface in the right panel.

In momentum space this is concentrated not only on the individual k_n , with contributions that are constant in \mathbf{r} , equal to the weights $|c_n|^2$ in (5.8), but also on the midpoints between pairs of k_n , with contributions that are real plane waves in \mathbf{r} , with wavevectors given by the differences of the corresponding pairs of k_n . These properties are illustrated in figure 2.

The second Wigner function is that representing a Gauss-modulated vortex of order m in the \mathbf{r} plane, for which, in polar coordinates

$$\psi(\mathbf{r}) = \frac{1}{\sqrt{\pi m!}} \exp\left(-\frac{1}{2}r^2\right) r^m \exp(im\phi). \tag{5.10}$$

The corresponding Wigner function is

$$W_m(\mathbf{r}, \mathbf{k}) = \frac{(-1)^m}{\pi^2} \exp(-(r^2 + k^2)) L_m((k_x - y)^2 + (k_y + x)^2), \tag{5.11}$$

in which the L_m are Laguerre polynomials [11], whose arguments can be written in the following alternative forms:

$$(k_x - y)^2 + (k_y - x)^2 = r^2 + k^2 + 2\mathbf{r} \times \mathbf{k} \cdot \mathbf{e}_z = |\mathbf{r} + \mathbf{k} \times \mathbf{e}_z|^2 = |\mathbf{k} - \mathbf{r} \times \mathbf{e}_z|^2. \tag{5.12}$$

To illustrate this Wigner function, we note that it is invariant under a simultaneous rotation of \mathbf{r} and \mathbf{k} , so it suffices to choose $\mathbf{k} = k_x \mathbf{e}_x$ and show W_m for different values of k_x , as in figure 3.

For the m th order vortex, it is not hard to calculate the local momentum starting from (5.10), with the (obvious) result

$$\mathbf{k}_{\text{Wigner}}(\mathbf{r}) = \frac{m}{r} \mathbf{e}_\phi. \tag{5.13}$$

To derive this, any of the preceding formulas can be used; the most immediate is probably the first equality in (2.1).

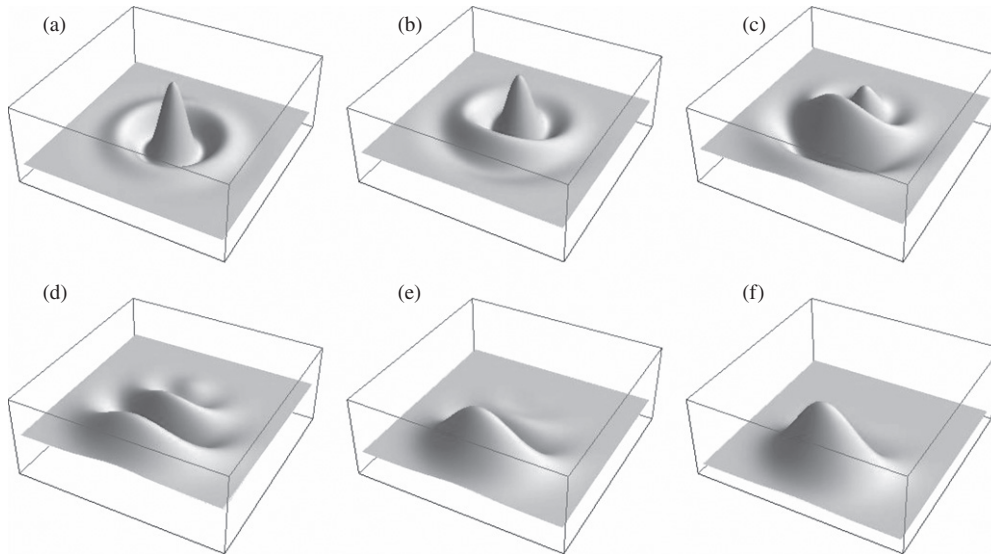


Figure 3. Wigner function $W_m(\mathbf{r}, \mathbf{k})$ (equation (5.11)) for $m = 4$, representing a wave with a fourth-order vortex, depicted in $\mathbf{r} = (x, y)$ space with $|x, y| \leq 3$ for $\mathbf{k} = k_x \mathbf{e}_x$, where, in (a)–(f), $k_x = (0 [0.5] 2.5)$.

6. Momentum 5: weak momentum with position postselected

This last of our five momenta makes contact with a wider circle of ideas, developed in recent decades by Aharonov and his collaborators [12–14]. They define a new class of quantum measurements, in which an operator \hat{A} is measured in a state $|\psi\rangle$ after ‘post-selection’ by a different state $|\phi\rangle$. If the measurement is made by weak coupling to a pointer, then in suitable circumstances [15] the pointer coordinate is shifted by the ‘weak value’

$$A_{\text{weak}} = \text{Re} \frac{\langle \phi | \hat{A} | \psi \rangle}{\langle \phi | \psi \rangle}. \quad (6.1)$$

(The imaginary value also has physical significance [16], not considered further here; it would correspond to the antisymmetrized version of (3.3).)

Choosing the operator \hat{A} as momentum $\hat{\mathbf{k}}$, and post-selecting with the position state $|\mathbf{r}\rangle$, leads to the local weak momentum

$$\mathbf{k}_{\text{weak}}(\mathbf{r}) = \text{Re} \frac{\langle \mathbf{r} | \hat{\mathbf{k}} | \psi \rangle}{\langle \mathbf{r} | \psi \rangle}. \quad (6.2)$$

Using (4.1), the last equality in (2.1), and the position representation, leads to the final equivalence:

$$\mathbf{k}_{\text{weak}}(\mathbf{r}) = \mathbf{k}_{\text{Wigner}}(\mathbf{r}) = \mathbf{k}_{\text{current}}(\mathbf{r}) = \mathbf{k}_{\text{local operator}}(\mathbf{r}) = \mathbf{k}_{\text{phase}}(\mathbf{r}). \quad (6.3)$$

This identification of local momentum as a weak value leads to additional insights, resulting from the observation that when the denominator in (6.1) is small the weak value of an operator can lie far outside the spectrum of \hat{A} [13]: the weak value can be ‘superweak’ [17, 18]. This is impossible with the conventional expectation (3.1), in which there is no post-selection. In the context of local momentum and the identification of \mathbf{k}_{weak} with $\mathbf{k}_{\text{phase}}$, superweakness means that the wave $\psi(\mathbf{r})$ can oscillate locally faster than any of the momenta

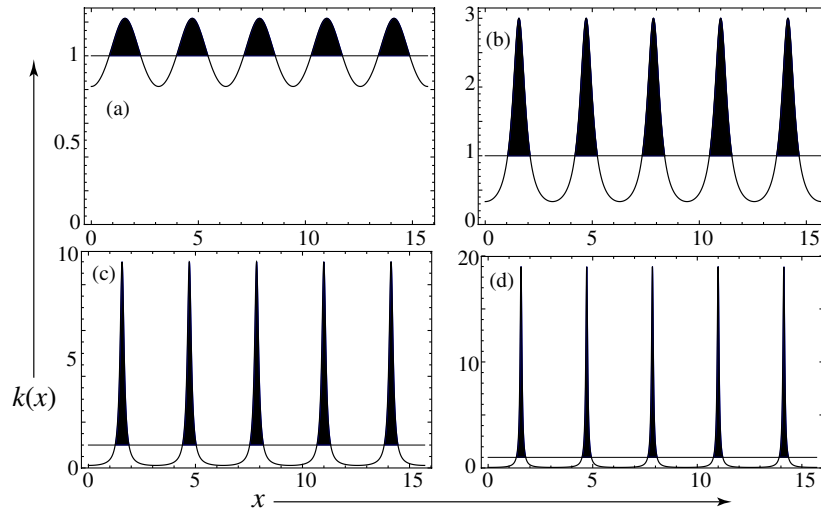


Figure 4. Local momentum (6.5) for the superposition (6.4), with the superoscillatory regions $k(x) > 1$ shaded, for (a) $a = 0.1$, (b) $a = 0.5$, (c) $a = 0.8$, (d) $a = 0.9$.

in the superposition of plane waves comprising it: it can ‘superoscillate’ [19–21]. And in view of the denominator in (6.2) we can anticipate that superoscillations can be extreme near the zeros (nodal manifolds) of $\psi(\mathbf{r})$.

Perhaps the simplest example is the superposition of two waves in $D = 1$:

$$\psi(x) = \exp(ix) + a \exp(-ix). \tag{6.4}$$

Here the spectrum of contributing momenta consists simply of the two points $k = \pm 1$. The local momentum, now denoted simply by $k(x)$ in view of the equivalences (6.3), and most easily calculated from (1.1), is (for a real)

$$k(x) = \frac{1 - a^2}{1 + a^2 + 2a \cos 2x}. \tag{6.5}$$

As figure 4 illustrates, this rises to large values at the minima of $|\psi|$ as a approaches unity; the values are

$$|k(x)|_{\max} = \left| \frac{1 + |a|}{1 - |a|} \right|. \tag{6.6}$$

When $a = 1$, the wave (6.4) is simply $\psi(x) = \cos x$, which is real, so as is well known, the local momentum is zero. Equation (6.5) reveals this as a singular limit: as a approaches unity, $k(x)$ approaches zero except for diminishing intervals surrounding the minima of $|\psi(x)|$ in which it is very large. In fact, the average value of the local momentum (6.5) is

$$k(x)_{\text{mean}} \equiv \frac{1}{\pi} \int_0^\pi dx k(x) = \text{sgn}(1 - |a|), \tag{6.7}$$

corresponding to the momentum of the dominant wave in the superposition.

Another example where local momentum gives unfamiliar insights into a familiar situation is the reflection and refraction of a monochromatic wave with wave number k_0 incident from vacuum on a refractive-index slab with index n (figure 5(a)). The local wavevector is shown in figures 5(c)–(e) for three values of refractive index, corresponding to the different

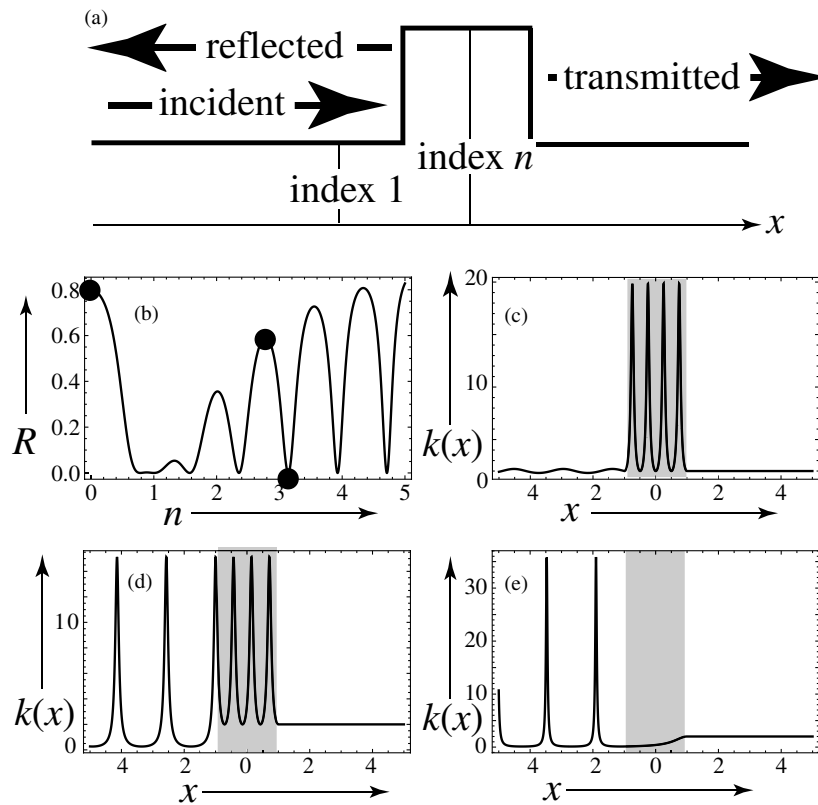


Figure 5. (a) Reflection and transmission of a monochromatic wave with wavenumber $k_0 = 2$ from a slab with refractive-index n between $x = \pm 1$. (b) Reflection intensity R as a function of n . Local wavenumber magnitudes for different refractive indices, indicated by filled circles in (b), are shown in (c) $n = 3.15$ (transmission resonance); (d) $n = 2.75$ (reflection maximum); (e) $n = 0$ (large reflection, wavefunction linear within the slab); the slab is indicated by the shaded regions in (c)–(e).

situations indicated in figure 5(b). This example shows superoscillation inside the slab whenever there are reflection or transmission resonances, and superoscillations when the reflection coefficient is large and there is strong interference between the incident and reflected waves.

The full richness of superoscillations associated with the local momentum emerges only for $D \geq 2$, because then it is typical for complex wavefunctions to possess zeros (cf figure 3), i.e. phase singularities at which $|\mathbf{k}|$ diverges and near which $\mathbf{k}(\mathbf{r})$ possesses a vortex structure. An illustration of this (discussed elsewhere [22, 23] with a different emphasis) is the following superposition of Bessel solutions of the Helmholtz equation in the plane with wavenumber k_0 (i.e. wavelength $2\pi/k_0$):

$$\psi(x, y) = J_m(k_0 r) \exp(im\phi) + \varepsilon J_0(k_0 r). \quad (6.8)$$

This is a perturbation of a wave which for $\varepsilon = 0$ possesses a vortex of order m at the origin. For finite ε , this splits into m vortices of order 1, as illustrated in figure 6. The superweak (i.e. superoscillatory) values of $\mathbf{k}(\mathbf{r})$ are illustrated in figure 7.

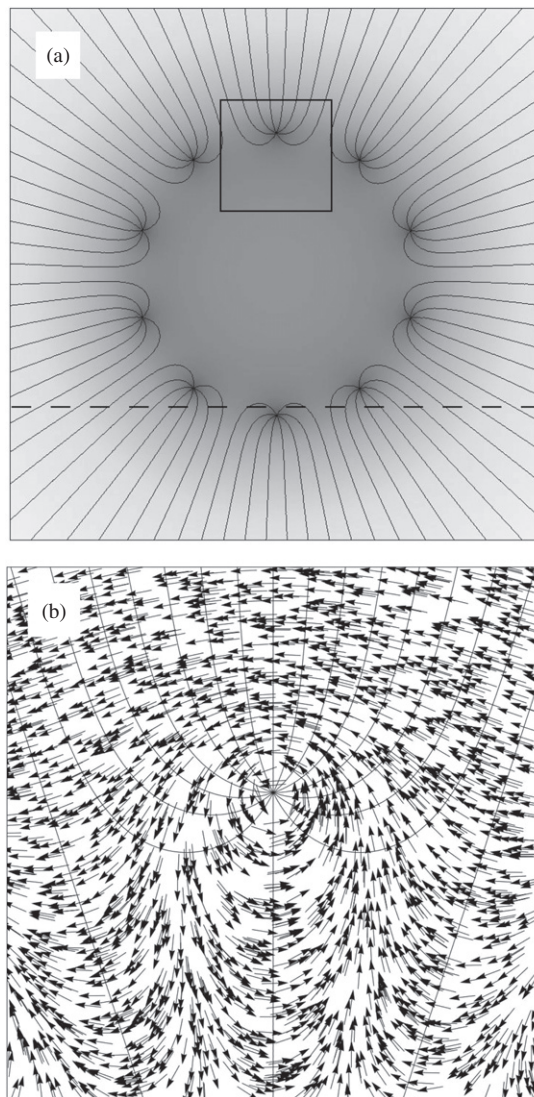


Figure 6. (a) The wave (6.8) with $m = 10$ and $\varepsilon = 10^{-7}$, shown for one square wavelength; the curves are wavefronts $\arg \psi = \text{constant} \pmod{2\pi}$ at intervals of $\pi/4$, and the shading indicates $\log |\psi|$ (black at the zeros of ψ). (b) Magnification of the square region indicated in (a), including the directions of the local momenta, shown as arrows.

Superoscillations are unexpectedly common in waves occurring naturally, for example, in monochromatic many-wave superpositions of the form (5.6), in which all \mathbf{k}_n have the same length k_0 and $N \gg 1$. These represent Gaussian random functions, for which the probability of a random point \mathbf{r} in the plane being superoscillatory, i.e. $|\mathbf{k}(\mathbf{r})| > k_0$, is $1/3$ [24], with similar values for $D > 2$ [25]. Another example, this time for $D = 1$, is superpositions (5.6) in which all the contributing plane waves are travelling forwards, i.e. all $k_{x,n} > 0$; nevertheless, there are substantial regions of the x axis for which the local momentum $k_x(x)$ is negative, i.e. flowing backwards [26].

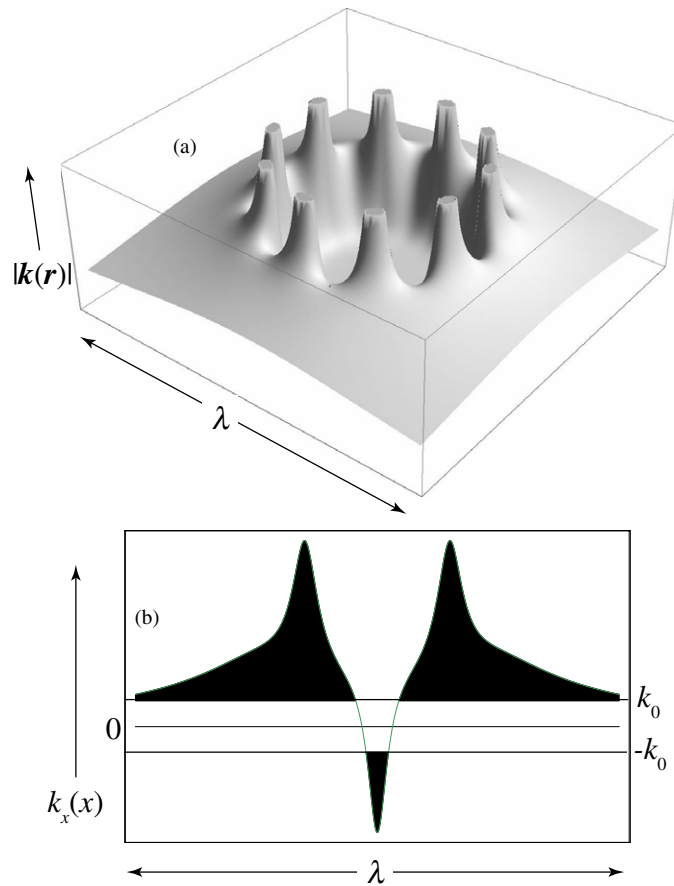


Figure 7. (a) As figure 6(a), showing the magnitude $|k(\mathbf{r})|$ of the local momentum, diverging at the phase vortices (zeros of $(\psi(\mathbf{r}))$). (b) local wavevector component $k_x(x)$ along the track shown as the dashed line in figure 6(a), close to three vortices, with the superoscillatory regions $|k_x| > k_0$ shaded.

7. Concluding remarks

A common pitfall is to think that in semiclassical or geometrical-optics regimes the local momentum $\mathbf{k}(\mathbf{r})$ that we have been studying corresponds to a classical trajectory or ray. This correspondence holds only when there is only one trajectory through \mathbf{r} . Usually—and almost always in bound systems—there are several trajectories, whose contributions are superposed and interfere. And since $\mathbf{k}(\mathbf{r})$ is a single-valued function it cannot represent them all. The reason can be stated succinctly, bearing in mind the phase gradient interpretation of section 4: the momentum in the superposition is not the superposition of the momenta. I have emphasized this elsewhere, with examples [3, 27, 28].

Momentum is often introduced through its connection with translation symmetry: in a homogeneous medium, momentum is conserved. But it is important to understand that this association does not hold for the local momentum $\mathbf{k}(\mathbf{r})$ considered here, because even in a uniform medium $\mathbf{k}(\mathbf{r})$ always varies with position (often in complicated ways, see figures 1 and 6); the only exception is the trivial case of a single plane wave.

It is clear that, as stated earlier, $\mathbf{k}(\mathbf{r})$ carries only part of the momentum distribution at the point \mathbf{r} . A complete description is contained in the Wigner function or any of its relatives, such as the Husimi. The latter has recently been processed in an imaginative way [29] to yield a pictorial representation of a series of local momenta \mathbf{r} , related in semiclassical cases to the momenta of classical trajectories through \mathbf{r} in cases where there are several.

We have represented all five momenta in terms of complex scalar waves in vacuum. However, similar formulas apply more generally, for example in vector wave optics. For paraxial light, where the electric field vector is represented by its helicity components ψ_+ and ψ_- , it is known [28, 30] that the orbital part of the transverse Poynting vector is

$$\mathbf{P}(\mathbf{r}) = \text{Im}[\psi_+^*(\mathbf{r})\nabla\psi_+(\mathbf{r})] + \text{Im}[\psi_-^*(\mathbf{r})\nabla\psi_-(\mathbf{r})], \quad (7.1)$$

in which ∇ denotes the gradient perpendicular to the propagation direction. The two contributions are both of the ‘current’ type (equation (4.2)). And for nonparaxial light the orbital Poynting vector is given by a slightly more general formula, involving the magnetic as well as the electric field [28, 31]. It would be interesting to investigate whether analogues of the five momenta can be constructed for waves of other types: relativistic particles governed by the Klein–Gordon and Dirac equations; crystal optics (i.e. anisotropic media); and left-handed (negative index) materials. In these more general situations, the different momenta might not be equal.

Finally, a natural question is: is $\mathbf{k}(\mathbf{r})$ observable? A suggestion that it might be comes from contrasting $\mathbf{k}(\mathbf{r})$ with the momentum current density $\mathbf{j}(\mathbf{r})$. These are two vectors with the same direction, simply related by (4.3). But they are physically very different. As we have seen, $\mathbf{k}(\mathbf{r})$ can be superweak: near phase vortices, it can greatly exceed the momenta in (for example) the plane waves comprising $\psi(\mathbf{r})$.

The weak value interpretation of section 6 suggests that these large values of $\mathbf{k}(\mathbf{r})$ could be momenta imparted to a small test particle (e.g. an atom) in the field $\psi(\mathbf{r})$, in individual quantum events; such events are rare because $\psi(\mathbf{r}) = 0$ at vortices. By contrast, $\mathbf{j}(\mathbf{r})$ is weighted by the additional factor $|\psi(\mathbf{r})|^2$ and so vanishes at vortices. In optics, $\mathbf{j}(\mathbf{r})$ corresponds to the Poynting vector, which is responsible for radiation pressure. This gives the average force on particles in the field, raising the possibility, envisaged earlier [28], that radiation pressure, when deconstructed into its individual quantum events, is the average over momentum transfers that are, near vortices, both large and rare. Simple calculations indicate that locating the test particle would involve a momentum uncertainty comparable with the superweak value to be detected; but this uncertainty would be random and isotropic, whereas the superweak momentum is precisely directed, suggesting the feasibility of this proposed way to detect it. Further study is in progress.

Acknowledgments

I thank Professor Stephen Barnett for directing me to [5], and Dr Mark Dennis for a helpful suggestion. My research is supported by the Leverhulme Trust.

References

- [1] Madelung E 1927 Quantentheorie in hydrodynamische form *Z. Phys.* **40** 322–6
- [2] Holland P 1993 *The Quantum Theory of Motion. An Account of the de Broglie–Bohm Causal Interpretation of Quantum Mechanics* (Cambridge: Cambridge University Press)
- [3] Berry M V 2002 Exuberant interference: rainbows, tides, edges, (de)coherence *Phil. Trans. R. Soc. Lond. A* **360** 1023–37
- [4] Newton I 1730 *Opticks: or a Treatise of the Reflections, Inflections and Colours of Light* 4th edn (Mineola, NY: Dover) (corrected 1952 reprint)

- [5] Landau L 1941 The theory of superfluidity of helium II *J. Phys. USSR* **V5** 71–80
- [6] Berry M V, Chambers R G, Large M D, Upstill C and Walmsley J C 1980 Wavefront dislocations in the Aharonov–Bohm effect and its water-wave analogue *Eur. J. Phys.* **1** 154–62
- [7] Messiah A 1962 *Quantum Mechanics* (Amsterdam: North-Holland)
- [8] Wigner E P 1932 *Phys. Rev.* **40** 749–59
- [9] Groenewold H J 1946 *Physica* **12** 405–60
- [10] Moyal J E 1949 *Proc. Camb. Phil. Soc.* **45** 99–124
- [11] DLMF 2010 *NIST Handbook of Mathematical Functions* (Cambridge: Cambridge University Press) (<http://dlmf.nist.gov>)
- [12] Aharonov Y, Albert D Z and Vaidman L 1988 How the result of a measurement of a component of the spin of a spin $1/2$ particle can turn out to be 100 *Phys. Rev. Lett.* **60** 1351–4
- [13] Aharonov Y and Rohrlich D 2005 *Quantum Paradoxes: Quantum Theory for the Perplexed* (Weinheim: Wiley-VCH)
- [14] Aharonov Y, Popescu S and Tollaksen J 2010 A time-symmetric formulation of quantum mechanics *Phys. Today* **63** 27–33
- [15] Berry M V and Shukla P 2012 Pointer supershifts and superoscillations in weak measurements *J. Phys. A: Math. Theor.* **45** 015301
- [16] Jozsa R 2007 Complex weak values in quantum measurement *Phys. Rev. A* **76** 044103
- [17] Berry M V and Shukla P 2010 Typical weak and superweak values *J. Phys. A: Math. Theor.* **43** 354024
- [18] Berry M V, Dennis M R, McRoberts B and Shukla P 2011 Weak value distributions for spin $1/2$ *J. Phys. A: Math. Theor.* **44** 205301
- [19] Berry M V 1994 Faster than Fourier *Quantum Coherence and Reality: in Celebration of the 60th Birthday of Yakir Aharonov* ed J S Anandan and J L Safko (Singapore: World Scientific) pp 55–65
- [20] Aharonov Y, Colombo F, Sabadini I, Struppa D C and Tollaksen J 2011 Some mathematical properties of superoscillations *J. Phys. A: Math. Theor.* **44** 365304
- [21] Berry M V and Popescu S 2006 Evolution of quantum superoscillations, and optical superresolution without evanescent waves *J. Phys. A: Math. Gen.* **39** 6965–77
- [22] Berry M V 2008 *Waves near zeros in Coherence and Quantum Optics* ed N P Bigelow, J H Eberly and C R J Stroud (Washington, DC: Optical Society of America) pp 37–41
- [23] Berry M V 2013 A note on superoscillations associated with Bessel beams *J. Opt.* **15** 044006
- [24] Dennis M R, Hamilton A C and Courtial J 2008 Superoscillation in speckle patterns *Opt. Lett.* **33** 2976–8
- [25] Berry M V and Dennis M R 2009 Natural superoscillations in monochromatic waves in D dimensions *J. Phys. A: Math. Theor.* **42** 022003
- [26] Berry M V 2010 Quantum backflow, negative kinetic energy, and optical retro-propagation *J. Phys. A: Math. Theor.* **43** 415302
- [27] Berry M V and McDonald K T 2008 Exact and geometrical-optics energy trajectories in twisted beams *J. Opt. A: Pure Appl. Opt.* **10** 035005
- [28] Berry M V 2009 Optical currents *J. Opt. A: Pure Appl. Opt.* **11** 094001
- [29] Mason D J, Boronda M F and Heller E J 2013 Quantum flux and reverse engineering of quantum wavefunctions *Europhys. Lett.* **102** 60005
- [30] Bekshaev A Y and Soskin M S 2007 Transverse energy flows in vectorial fields of paraxial beams with singularities *Opt. Commun.* **271** 332–48
- [31] Bliokh K Y, Bekshaev A Y and Nori F 2013 Dual electromagnetism: helicity, spin, momentum and angular momentum *New J. Phys.* **15** 033026